THE ROYAL SOCIETY

Global geomagnetic field models for the past 3000 years: transient or permanent flux lobes?

By Catherine G. Constable[1], Catherine L. Johnson[2] and Steven P. Lund[3]

[1]*Institute for Geophysics and Planetary Physics, Scripps Institution of Oceanography, University of California at San Diego, La Jolla, CA 92093-0225, USA* (cconstable@ucsd.edu)

[2]*Department of Terrestrial Magnetism, Carnegie Institution of Washington, 5241 Broad Branch Road, Washington, DC 200015, USA* (cjohnson@dtm.ciw.edu)

[3]*Department of Earth Sciences, University of Southern California, Los Angeles, CA 90089-0740, USA* (slund@usc.edu)

PSVMOD1.0 is a compilation of globally distributed palaeodirectional data from archaeomagnetic artefacts, lava flows, and lake sediments at 24 sites evaluated at 100 year intervals from 1000 BC to AD 1800. We estimate uncertainty in these measures of declination and inclination by comparison with predictions from standard historical models in time-intervals of overlap, and use the 100-year samples and their associated uncertainties to construct a sequence of minimum structure global geomagnetic field models. Global predictions of radial magnetic field at the core–mantle boundary (CMB), as well as inclination and declination anomalies at the Earth's surface, provide an unprecedented view of geomagnetic secular variations over the past 3000 years, and demonstrate a consistent evolution of the field with time. Resolution of the models is poorest in the Southern Hemisphere, where only six of the 24 sites are located, several with incomplete temporal coverage. Low-flux regions seen in the historical field near the North Pole are poorly resolved, but the Northern Hemisphere flux lobes are clearly visible in the models. These lobes are not fixed in position and intensity, but they only rarely venture into the Pacific hemisphere. The Pacific region is seen to have experienced significant secular variation: a strong negative inclination anomaly in the region, like that seen in 0–5 Ma models, persists from 1000 BC until AD 1000 and then gradually evolves into the smaller positive anomaly seen today. On average between 1000 BC and AD 1800, the non-axial-dipole contribution to the radial magnetic field at the core–mantle boundary is largest in the north-central Pacific, and beneath Central Asia, with clear non-zonal contributions. At the Earth's surface, average inclination anomalies are large and negative in the central Pacific, and most positive slightly to the east of Central Africa. Inclination anomalies decrease with increasing latitude. Average declinations are smallest in equatorial regions, again with strong longitudinal variations, largest negative departures are centred over Australia and Eastern Asia. Secular variation at the Earth's surface is quantified by standard deviation of inclination and declination about their average values, and at the CMB by standard deviation in radial magnetic field. All three show significant geographical variations,

but appear incompatible with the idea that secular variation in the Pacific hemisphere is permanently attenuated by greatly enhanced conductivity in D^{ω} beneath the region.

Keywords: geomagnetic secular variation; palaeomagnetism; geomagnetic field modelling

1. Introduction

Analyses of the historical record of the geomagnetic field provide an ever-improving (see Jackson *et al.*, this issue) view of the geomagnetic secular variation at the Earth's surface, as well as images of the radial component of the field downward continued to the core–mantle boundary (CMB). This record is well characterized for the time-interval AD 1840–1980 by the UFM1 model time-varying field of Bloxham & Jackson (1992). Historical measurements are sparse before AD 1600, so, for a global perspective, we must turn to the palaeomagnetic and archaeomagnetic record. Considerable effort has been devoted to assembling datasets that span the last 5 Myr (Quidelleur *et al.* 1994; Johnson & Constable 1996; McElhinny & McFadden 1997), and a number of field models have been published using lava flow directional data, as well as those from marine sediments and the limited palaeointensity measurements available for lava flows (Gubbins & Kelly 1993; Kelly & Gubbins 1997; Carlut & Courtillot 1998; McElhinny *et al.* 1996*a*, *b*; Johnson & Constable 1995, 1997, 1998; Schneider & Kent 1988, 1990).

The intermediate time-scales of hundreds to thousands of years have, to date, received less attention in terms of global modelling, because of more stringent age control requirements (compared with the temporal control needed for data spanning longer time intervals) and because the palaeomagnetic time-series used must be consistent over continent-sized regions. Regional studies have been published by Lund (1996), and, more recently, two globally distributed datasets have been compiled. Daly & Le Goff (1996) have produced model time-series from globally distributed archaeomagnetic observations for the last 2000 years; these have been the subject of study by Hongre *et al.* (1998). Lund & Constable (2000) have produced model time-series (PSVMOD1.0) of declination and inclination evaluated at 100-year intervals from 1000 BC to AD 1800. This compilation is not restricted to archaeomagnetic records, but includes lake sediments and lava flows, where there are appropriate quality and age controls. PSVMOD1.0 is used here to produce a series of 29 magnetic field models at 100-year intervals. Both the dataset and resulting models are accessible on the World Wide Web at http://mahi.ucsd.edu/cathy/Holocene, or via anonymous ftp at ozzy.ucsd.edu.

The models presented in this paper are compared with some derived earlier from both historical and longer-term palaeomagnetic data. Figure 1 shows predictions from UFM1 (Bloxham & Jackson 1992) averaged over the time-interval AD 1840–1980, LSN1, a time-averaged field model derived from 0–5 Ma lava flow directional data (Johnson & Constable 1997), and ALS3K, a time-averaged model for the past 3000 years derived from PSVMOD1.0 (Johnson & Constable 1998). The first column shows the radial component of the magnetic field at the CMB, while the second column is the non-axial-dipole part of the radial component: this second column is useful because the dominant axial dipole tends to obscure structure in the rest of

the field, particularly when it has been averaged over thousands of years. The third column of figure 1 is the inclination anomaly (the difference between the predicted inclination and that of a geocentric axial dipole for the site), and the rightmost column is the average declination. In our new models we have not used intensity information, thus, we have estimates of the field models to within an arbitrary scalar multiplier (disregarding other issues of non-uniqueness, see Proctor & Gubbins (1990) and Hulot *et al.* (1997)). We resolve this ambiguity by arbitrarily setting g_1^0 to be 30 μT, a value representative of the present field.

The historical field has been described in detail in Bloxham *et al.* (1989). The radial field at the CMB (figure 1*a*) contains four main static flux lobes that make a major contribution to the dipole part of the field. Minor changes occur in the lobes over the 140-year period, but no persistent drift. There is a region of low flux over the North and possibly also the South geographic Pole. The flux concentration in the central Pacific appears remarkably stable, as does a large low-flux region to the north and northwest of it. Persistent small changes occur to the east of the central Pacific concentration, but there is little large-scale drift in the Pacific hemisphere. The low-flux patch near Easter Island also appears permanent on this time-scale. In contrast with the Pacific hemisphere, the Atlantic hemisphere shows large reverse-flux patches, beneath the Southern Atlantic and Indian Oceans, that change rapidly with time and drift westward. The average field over this time is approximately antisymmetric about the Equator with the exception of the central Pacific flux concentration (note from 1*b* that this remains somewhat true even when the strongly antisymmetric dipole contribution to the field is removed). The Northern Hemisphere flux lobes are also seen in the non-axial-dipole B_r. Walker & Backus (1996) have shown that the present non-dipole field as measured by $\int B_r^2 \, \mathrm{d}^2S$ in the Pacific hemisphere is anomalously low compared with that in the Atlantic. The inclination anomaly (figure 1*c*) ranges from -24.0° to 26.4° with largest magnitude in equatorial to mid-southern latitudes, except in the Pacific region, where it is generally smaller than elsewhere. Average declinations are largest near the poles (a geometric effect), dominantly positive over the Pacific region, much of the Americas, central Asia and Australia, but negative in Europe, Africa the Atlantic and Indian Oceans. Although declination anomalies are small in the central Pacific as well as over eastern Asia, it does not seem that they are exceptional when compared with some other locations.

In contrast to the historical model, ALS3K and LSN1 show only small, but nonetheless significant, departures from predictions of the geocentric axial-dipole hypothesis. Over 3000 years, secular variation results in average inclination and declination anomalies (figure 1*g*, *h*) that exhibit about half the range seen in UFM1. Interestingly, the spatial structure of these anomalies is also quite different, indicating that many of the features seen in UFM1 are far from permanent. The largest inclination anomalies over this time-interval are strong negative anomalies in the central Pacific, and the declination anomaly has a completely different structure. Although there is a strong suggestion of the static flux lobes in the radial magnetic field, they are not well resolved by the model: Johnson & Constable (1998) showed that 1980 data similar to PSVMOD1.0 in distribution and accuracy inverted for the 1980 field will resolve structure like that in ALS3K when flux lobes are present. We note here that ALS3K was derived from temporal averages of the directional data: this average will inevitably be somewhat biased by gaps in the available time-series for PSVMOD1.0.

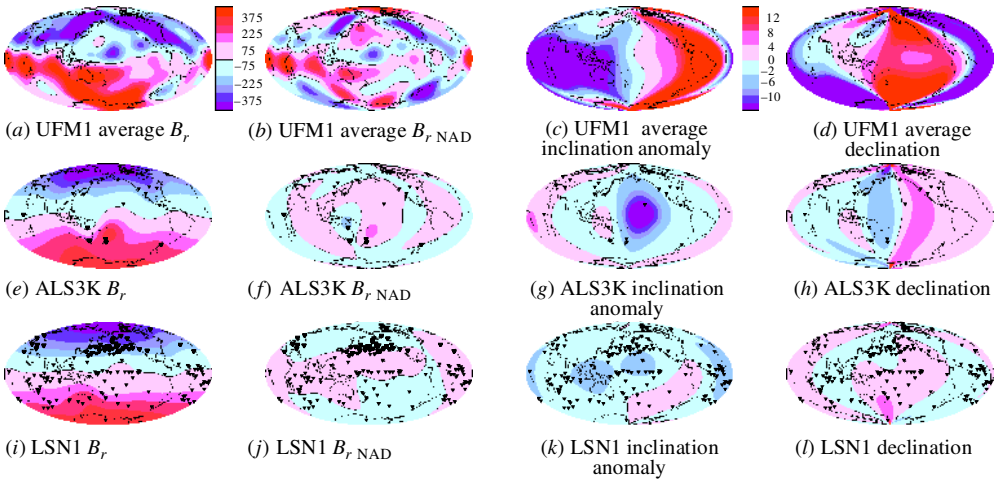

Figure 1. Radial magnetic field at CMB (B_r), radial non-axial-dipole magnetic field at CMB ($B_{r\,\mathrm{NAD}}$), inclination anomalies, and declination for UFM1 after averaging over the AD 1840–1980 time-interval (*a*)–(*d*), for ALS3K (*e*)–(*h*), and for LSN1 (*i*)–(*l*). Radial field maps are in mT (contour interval 75 mT), inclination anomaly and declination maps are in degrees (contour interval 2°).

The 0–5 Ma model LSN1 is more attenuated in structure than ALS3K, reflecting that, over long time-intervals, the geomagnetic field structure is closer to that predicted from an axial dipole. Nonetheless, there is non-zonal (longitudinal) structure in the field: the observations cannot be adequately fitted by a purely axisymmetric model. Simulations show that the Northern Hemisphere flux lobes are difficult to detect in inversions of 1980 data similar to the 0–5 Ma normal polarity dataset in distribution and accuracy. Thus, it remains plausible from ALS3K and LSN1 that the flux lobes are indeed quasi-permanent features in the geomagnetic field. Predictions from the minimum structure model LSN1 show predominantly negative inclination anomalies ranging from −8° in the central Pacific to +2° in the southeastern Pacific. Large inclination anomalies tend to be in the equatorial and mid-latitude regions, which is also where the sampling sites are most concentrated. Declination anomalies are generally positive over Europe, Africa and Western Asia, as well as in much of the Pacific. Johnson & Constable (1998) drew attention to similarities in the average radial magnetic field at the CMB in the Pacific region in ALS3K and LSN1: in the surface field this is manifest in the significant negative inclination anomaly. Declination predictions are less similar. This should not be surprising since the declination is most sensitive to B_r in regions on the CMB that are displaced by 22° in longitude from the sampling site (see, for example, Johnson & Constable 1997, 1998), and sampling of the CMB by the ALS3K and LSN1 datasets is quite different (Johnson & Constable 1998).

Part of the motivation for developing the models described above is a longstanding question about the geomagnetic field recently enunciated by Gubbins (1998) in the form of two competing theories. Theory 1 holds that, since we mostly see westward drift at the Earth's surface during historical times, non-axisymmetric parts of the field will be averaged out over time to leave a purely axisymmetric average (see,

for example, McElhinny *et al.* 1996*b*; Carlut & Courtillot 1998). Theory 2 draws on recent analyses of historical secular variation (Bloxham *et al.* 1989; Bloxham & Jackson 1992) in which it is observed that westward drift is confined to one part of the core surface: there is no tendency to drift through a full rotation, and little secular variation in the Pacific. This may be interpreted as evidence that the core is influenced by the solid mantle resulting in a non-axisymmetric contribution to the time-averaged geomagnetic field. Over 5 Myr or even 3 kyr, the departures of the time-averaged field from axisymmetry are small, and, because of limitations in the datasets, both theory 1 and theory 2 remain plausible interpretations of the time-averaged field structure (Carlut & Courtillot 1998; Gubbins & Kelly 1993; Kelly & Gubbins 1997; Johnson & Constable 1995, 1997, 1998). However, the dataset to be described in the next section allows the development of models at 100-year intervals. Judging from UFM1, the signal over such 100-year time-intervals should be large in comparison with the results of figure 1*e–l*, and, despite the rather sparse global distribution of sites, there remains the facility to track any possible evolution of the flux lobes, and apparently unusual Pacific secular variation. The resolution of this longstanding question of the influence of the lower mantle on the geodynamo from the perspective of field behaviour consistent with palaeomagnetic data is important. Three-dimensional numerical simulations of the geodynamo investigating different spatial variations in heat flow across the CMB are already being carried out (Glatzmaier *et al.* 1999; Bloxham 1998), and independent investigations focusing on the properties of palaeomagnetic datasets provide important ground truthing for such simulations. Furthermore, if heat-flow patterns across the CMB influence geodynamo processes, there are implications for the geomagnetic field over longer time-scales than the past 5 Myr, since the thermal structure of the lower mantle has certainly changed over time-scales of 10^7 to 10^8 yr (Richards & Engebretson 1992; Lithgow-Bertelloni & Richards 1998). Greatly enhanced electrical conductivity in D^{ω} beneath the Pacific region (see, for example, Runcorn 1992) has also been considered as a possible mechanism for attenuating geomagnetic secular variations at the Earth's surface and influences on virtual geomagnetic pole (VGP) paths during reversals. Further examinations of the influence of electromagnetic torques on the mantle due to the poloidal field led, initially, to suggestions that heterogeneity in mantle conductivity is a plausible mechanism (Arnou *et al.* 1996) to influence the trajectory of the VGP during reversals. Later work with a more complete consideration of the problem led to a reversal of this opinion (Brito *et al.* 1999). Most recently, Holme (2000) has argued that the conductance required for such a mechanism is inconsistent with the observed core–mantle angular momentum exchange on decadal time-scales.

In what follows, we briefly review the PSVMOD1.0 dataset described in detail by Lund & Constable (2000) and the methodology for constructing models (also described elsewhere; see Johnson & Constable (1995, 1997)). We present 'snapshots' of the geomagnetic field—models at 100-year intervals—and discuss the evolution and secular variations of features observed both at the CMB and at the Earth's surface.

2. The PSVMOD1.0 dataset

PSVMOD1.0 consists of model time-series at 24 globally distributed sites (locations indicated by the triangles on figure 1*e–h*, each of which contribute palaeomagnetic

Table 1. *Sites contributing to the field models for the periods 1000 BC to AD 1800*

code	latitude	longitude	class
WUS	35.0° N	250.0° E	1A
JPN	35.0° N	135.0° E	1A
SEU	40.0° N	20.0° E	1A
UKR	50.0° N	30.0° E	1A
WUR	50.0° N	0.0° E	1A
HAW	20.0° N	205.0° E	1B
MAM	17.0° N	265.0° E	1B
PRC	35.0° N	115.0° E	1B
CAU	40.0° N	45.0° E	1C
NZE	35.8° S	174.9° E	2A
AUS	38.0° S	145.0° E	2B
MON	46.0° N	106.0° E	2C
BAI	52.4° N	106.1° E	3A
FIS	42.6° N	241.4° E	3A
ICE	66.0° N	337.0° E	3A
KEI	38.2° S	142.9° E	3A
LEB	41.9° N	280.1° E	3A
LLO	56.1° N	355.3° E	3A
LSC	45.0° N	267.2° E	3A
POU	41.3° S	175.2° E	3A
VUK	63.4° N	28.6° E	3B
ARG	41.0° S	288.5° E	3B
EAC	17.3° S	106.1° E	3B
TUR	2.6° N	36.6° E	3C

records of declination and inclination at 100-year intervals when available). Each time-series was developed from composite archaeomagnetic or sediment palaeosecular variation data with independent good-quality age control. Where ^{14}C dating was used in the original studies, the time-scale has been transformed to calendar years using the calibration of Clark (1975). Lund & Constable (2000) classified data for each time-series as follows.

Class 1: archaeomagnetic directional records with sufficient data to characterize the pattern of field variability.

Class 2: fragmentary archaeomagnetic data (inclination-only, short-duration, large data gaps).

Class 3: sediment directional records.

It is assumed that the lower the number of the record type, the better the data quality. Relative data quality within each record type was also indicated by a letter between A and D, with A indicating the best quality records. We note that these classifications are purely qualitative, and, in attempting to assign numerical uncertainties to PSVMOD1.0 for use in our later inversions, we have made an independent assessment based on comparisons with historical data. Table 1 gives the site locations and the classification codes for each site, and the temporal completeness of the

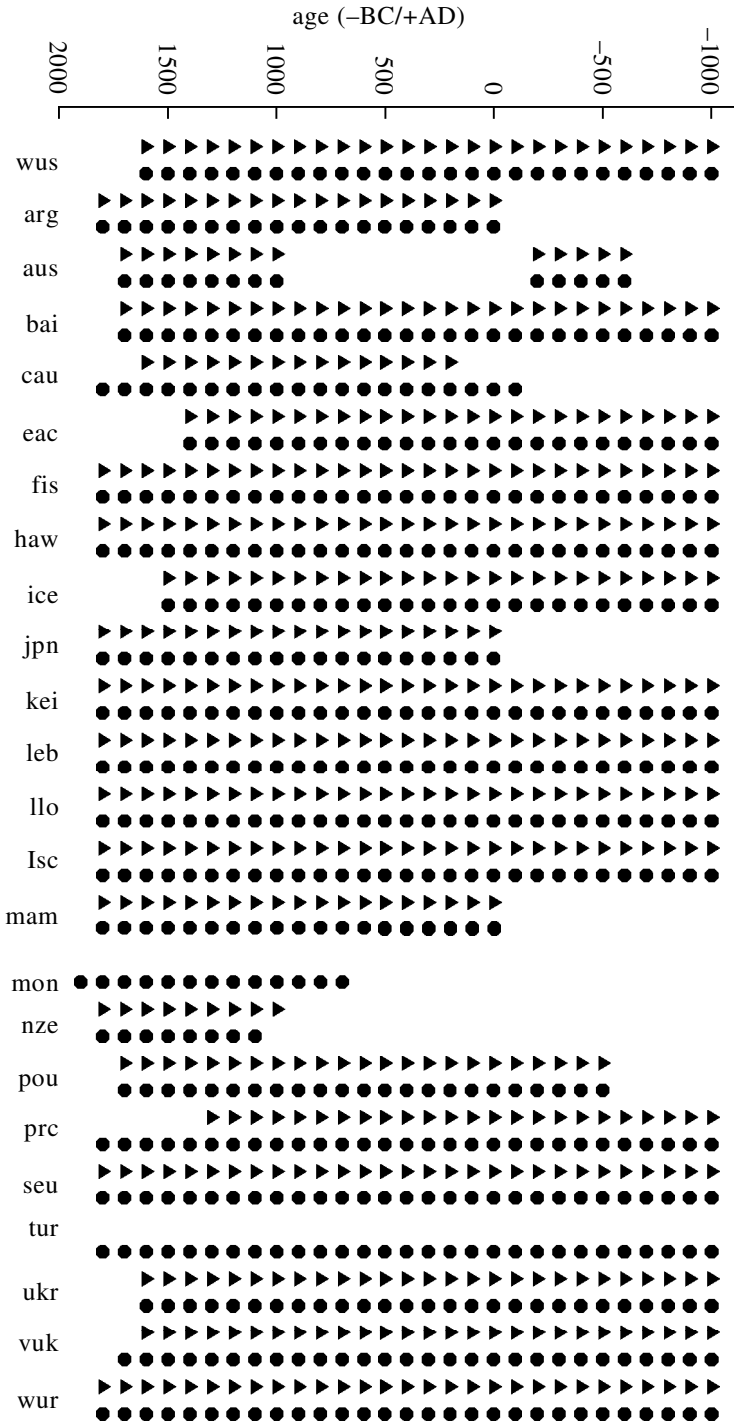

Figure 2. Temporal sampling at each site: a triangle (circle) at the time point indicates the existence of a 100-year sample of declination (inclination) at the indicated site.

records is shown in figure 2, where a triangle at a given time above the site code indicates the existence of a 100-year sample for declination, and a circle indicates inclination. The 100-year sample is not a direct average of the field direction over the 100-year interval, but an evaluation at the indicated time based on a composite curve from multiple observations. In general, each 'datum' represents something like a 20–30-year average of the field depending somewhat on the dating resolution and the general quality of the record. Age uncertainty is generally larger for sediments than for archaeomagnetic sites. We note that the coverage in the Southern Hemisphere is very sparse for some time-intervals; a point to be kept in mind in evaluating the models derived in the next section.

Lund & Constable (2000) discuss the possible causes of uncertainty in the PSVMOD1.0 directions in some detail. There are five sources of uncertainty in our observations:

(i) error in the field direction recorded by the rock sample on acquisition of depositional or thermal remanence;

(ii) contamination of the direction from the core field by local magnetic field anomalies;

(iii) uncertainty in the age at which magnetic remanence was acquired;

(iv) orientation errors during sampling; and

(v) inadequate magnetic cleaning in the palaeomagnetic laboratory such that the characteristic remanence direction may not be recovered.

The combined influence of these processes can be estimated by comparing PSVMOD1.0 with corresponding predictions from Bloxham & Jackson's (1992) UFM in the post-AD 1690 time period. Sixteen sites have directions for AD 1800, and 20 for AD 1700; the archaeomagnetic sites tend to have more complete records in the very recent past, because the top of lake-sediment cores is often disturbed in the coring process. Absolute orientation of the archaeomagnetic samples also tends to be more accurate, because it is rare for absolute records of declination to be acquired during coring. The average deviation for all sites from UFM is close to zero, and, using the available comparisons, standard errors of 2.5° were assigned to both declination and inclination measurements derived from archaeomagnetic sources, while for lake sediments standard errors of 3.5° and 5.0° were assigned to inclination and declination, respectively. Experimentation suggests that in general the largest source of uncertainty in our observations is the secular variation itself, which, combined with uncertainties in age, can contribute the major part of the observed deviation from UFM predictions.

Lund & Constable (2000) plot average declination and inclination anomalies for PSVMOD1.0 relative to a geocentric axial dipole, and compare them with similar site residuals for both UFM and LSN1. The signal in PSVMOD1.0 is generally intermediate in magnitude between that in UFM and LSN1, reflecting the time-scale over which the various records are averaged. All models show coherent spatial structures in the residuals over areas several thousand kilometres across, but there are some significant differences between these structures over the three time-intervals represented here. For example, at TUR in Kenya, PSVMOD1.0 exhibits a positive inclination

Table 2.

epoch	iteration no.	starting RMS	final RMS	% variance reduction	model norm
AD 1800	05	3.02	1.00	89.0	1.30
AD 1700	07	2.40	1.00	82.6	1.93
AD 1600	14	2.38	1.00	82.3	3.28
AD 1500	08	2.20	1.52	52.3	1.40
AD 1400	11	1.99	1.27	59.3	1.66
AD 1300	09	2.08	1.30	60.9	1.36
AD 1200	07	2.66	1.38	73.1	1.92
AD 1100	07	3.08	1.42	78.7	3.06
AD 1000	07	3.19	1.39	81.0	2.13
AD 900	09	2.89	1.44	75.2	1.65
AD 800	09	2.33	1.23	72.1	1.08
AD 700	09	2.54	1.57	61.8	2.15
AD 600	09	2.79	1.90	53.6	1.85
AD 500	11	2.51	1.54	62.4	1.58
AD 400	09	2.26	1.45	58.8	1.44
AD 300	08	2.12	1.35	59.4	1.67
AD 200	06	2.17	1.41	57.8	1.29
AD 100	09	2.00	1.31	57.1	1.74
AD 0	08	2.28	1.67	46.4	2.09
100 BC	07	2.43	1.79	45.7	1.67
200 BC	17	2.32	1.55	55.4	2.15
300 BC	07	2.89	1.80	61.2	2.02
400 BC	05	3.09	1.79	66.4	1.81
500 BC	07	3.97	2.15	70.7	2.41
600 BC	07	4.53	2.14	77.7	3.18
700 BC	03	5.28	2.93	69.2	2.98
800 BC	03	5.26	2.51	77.2	3.50
900 BC	04	4.71	2.36	74.9	2.74
1000 BC	05	3.72	1.87	74.7	2.05

anomaly, while both LSN1 and UFM show negative values. While we cannot rule out the possibility of some systematic errors in PSVMOD1.0, and we can certainly look for improved geographic and temporal coverage in the future, the analyses of Lund & Constable (2000) demonstrate good regional coherence and general reliability of the time-series.

3. Models

The detailed evaluation of the archaeomagnetic dataset described in Lund & Constable (2000), and summarized in the previous section, permits the investigation of the evolution of the global geomagnetic field over the past 3000 years. Figure 1 shows that the recent time-averaged structure of the field, as seen in UFM1, is quite different from that for the past 3 kyr, and, thus, we might expect significant changes in global field behaviour. Spherical harmonic models of the geomagnetic field were con-

structed at 100-year intervals using data from as many sites as are available (figure 2) at each time-interval. The modelling procedure follows that used in the generation of time-averaged field models for the periods 0–5 Ma and 0–3 Ka, and details can be found elsewhere (Johnson & Constable 1995, 1997, 1998). The scalar geomagnetic potential is described in terms of a spherical harmonic expansion, and, thus, our measurements of declination and inclination are nonlinearly related to the spherical harmonic coefficients, which are the model parameters. We use an iterative nonlinear inversion procedure, modified for geomagnetic field modelling from Constable *et al.*'s (1987) Occam's inversion algorithm; our models are regularized by minimizing the mean square value of the non-axial-dipole part of the radial magnetic field (B_r) at the CMB while fitting the data to a specified tolerance. As discussed by Johnson & Constable (1997) in the context of constructing LSN1, our model choice depends critically upon the minimum acceptable misfit to our observations, designated in the previous section. Under the assumption that these uncertainties are independent, zero-mean, Gaussian variables, the target misfit of the model to our data will correspond to the expected value of χ^2_N, which is N when the misfit is normalized by the data uncertainties. In practice, the target value for the misfit was not always attainable without generating overly complicated field models: we therefore compromise and select models with a plausible degree of roughness, and a slightly higher misfit to the observations. The necessity for this probably indicates that our use of UFM to calibrate the uncertainties in PSVMOD1.0 is not adequate to deal with variations in data quality as they extend further into the past. Table 2 lists the initial RMS signal in the data (measured relative to GAD, and normalized by the standard error), the RMS of the final model, the percentage variance reduction, the roughness of the final model (model norm) for each epoch, and the iteration at which the preferred model was achieved. The variance reductions achieved range from 46 to 89%, and are typically *ca.* 70%. The model norm does not contain the axial-dipole contribution to the roughness, and is normalized relative to that contribution.

The sequence of models from 1000 BC to AD 1800 is presented in figure 3, using the same format as in figure 1: note, however, that the non-axial-dipole contribution to B_r at the CMB ($B_{r_{\mathrm{NAD}}}$) is on a different colour scale. There is clearly a coherent temporal evolution of these field models with structures persisting for hundreds of years and gradually evolving into new features. Since each model is a snapshot in time, and independent of the data in adjacent temporal slots, this reflects well on the quality of the observations and the care taken in selecting them. There is significant, evolving non-zonal structure in the field models, whose character appears quite distinct in the different representations of the field. B_r at the CMB is dominated by the axial-dipole field contribution, but changes in field structure can be seen: these are revealed more clearly in the second column of figures, from which the axial-dipole contribution has been subtracted. From this we see that from 1000 BC until 600 BC the flux lobe over Asia was dominant and there was a positive anomaly in $B_{r_{\mathrm{NAD}}}$ over western North America extending across the Pacific past Hawaii. The North American flux lobe is only occasionally visible during this time. Southern Hemisphere field structure is very smooth, reflecting the paucity of data there. Large negative inclination anomalies in the central Pacific region, and positive ones centred in the Indian Ocean, are associated with these structures. The focus of these inclination anomalies in different geographic regions from the radial field anomalies reflects the different CMB sampling kernels for the radial field, inclination and declination.

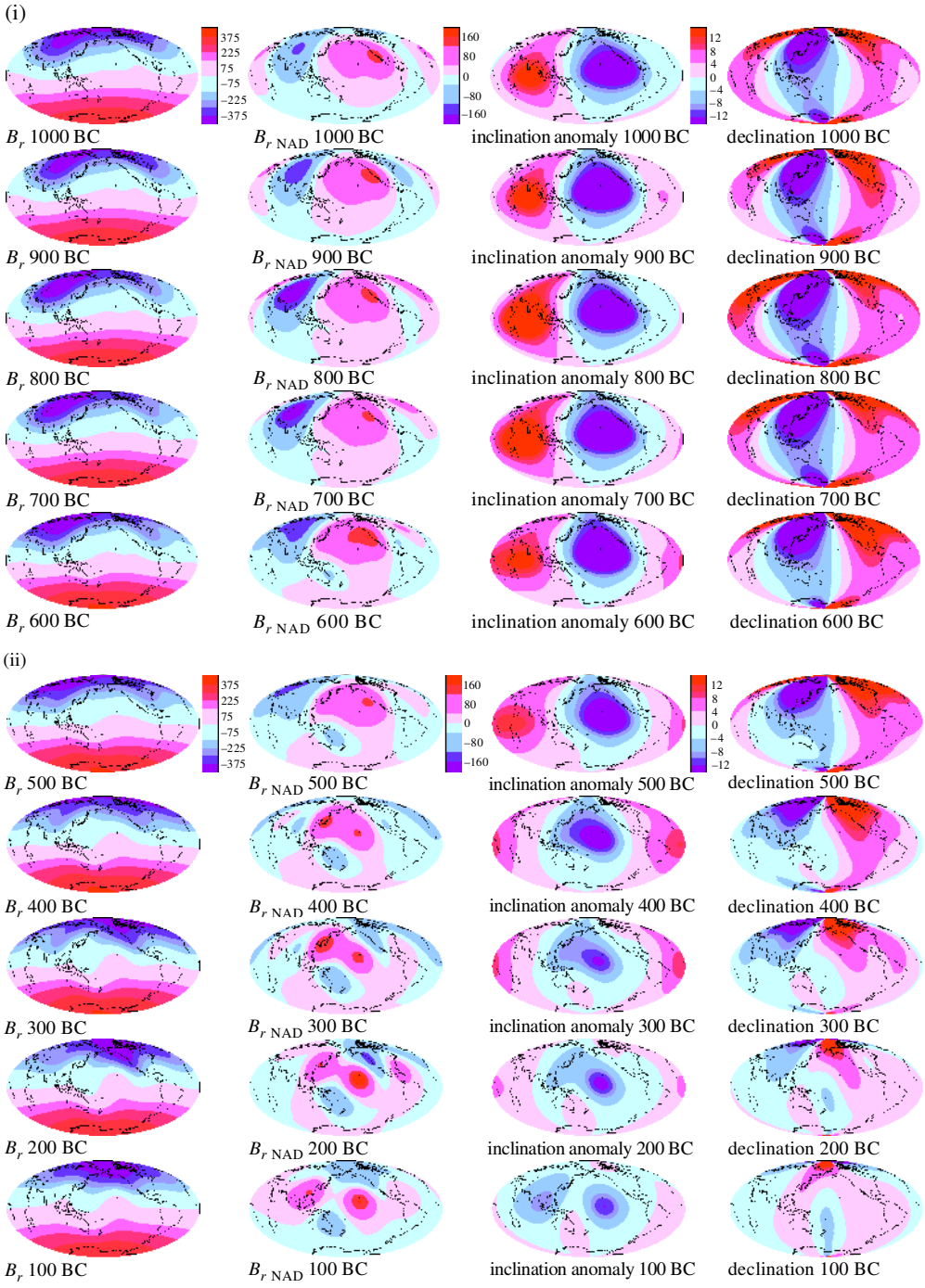

Figure 3. Snapshots of B_r (75 mT contour interval), $B_{r_{\mathrm{NAD}}}$ (40 mT contour interval), inclination anomaly at the Earth's surface, and declination (contour interval 2°) for models every 100 years from 1000 BC to AD 1800. Colour bars sit to the right of the parameter plotted except for the declination, which has the same scale as the inclination.

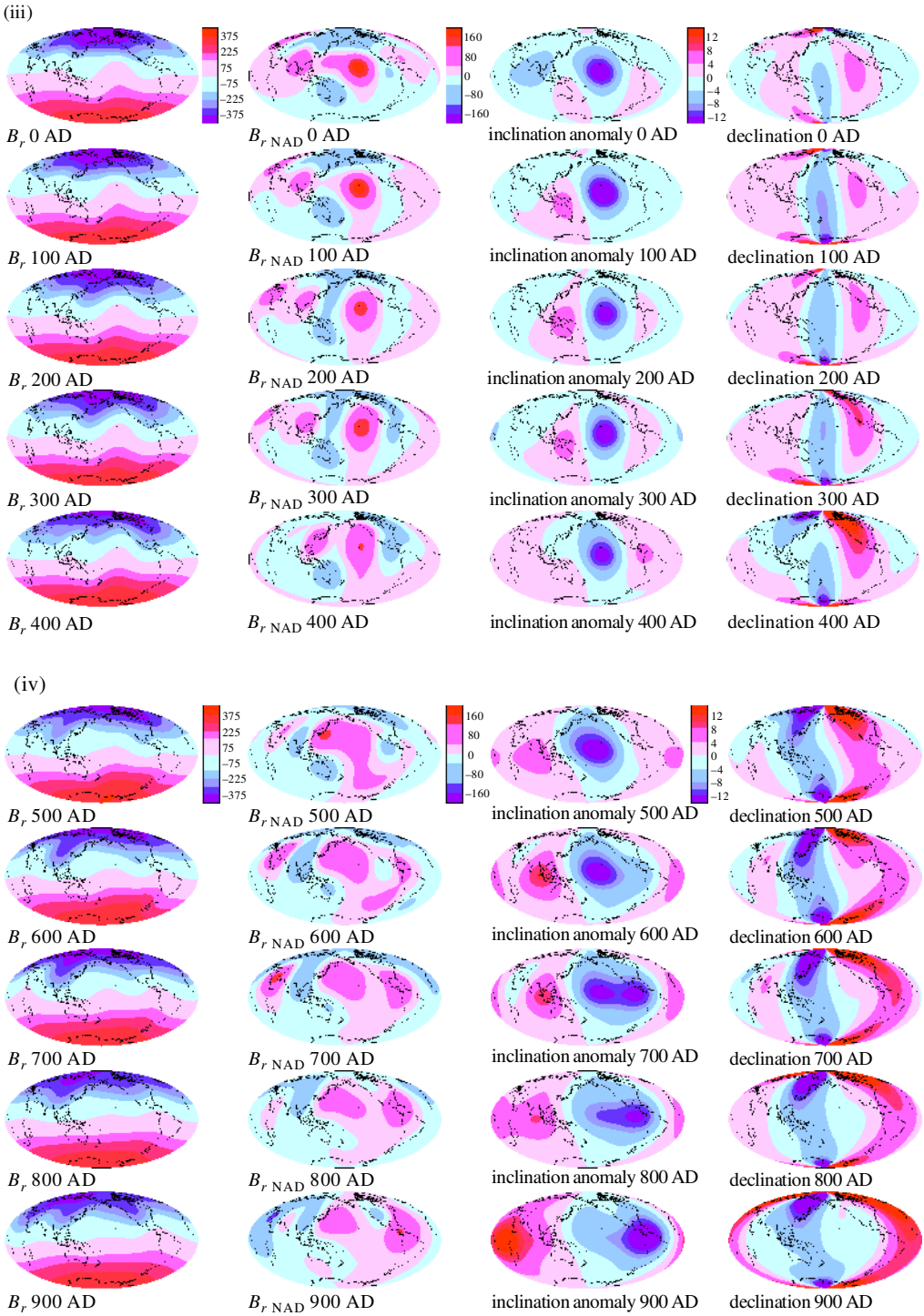

Figure 3. (*Cont.*)

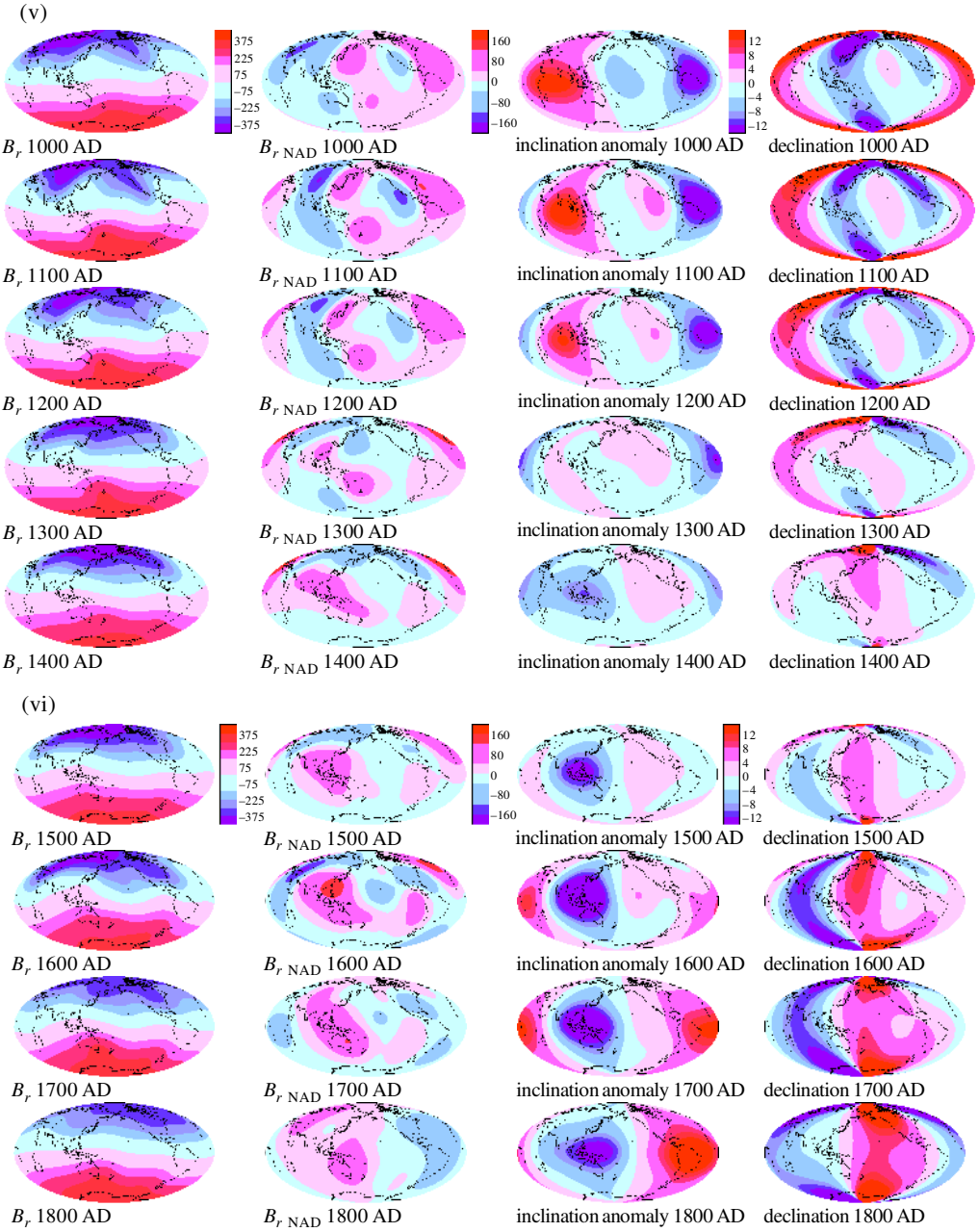

Figure 3. (*Cont.*)

At about 500 BC, the influence of the Asian flux lobe begins to wane, the positive focus of $B_{r_{\mathrm{NAD}}}$ shifts to the western Pacific, but still encompasses the region beneath Hawaii, and a negative lobe develops over North America with a finger extending into the Atlantic region. A negative focus centred northwest of New Zealand develops, perhaps because of evolving field structure, although it may reflect the addition of

New Zealand lake-sediment data to the available dataset (see figure 2). Negative inclination anomalies weaken somewhat and spread into eastern Asia and the Atlantic, forming a pair of foci over India and the Pacific by 100 BC. By 100 BC, the North American flux lobe in $B_{r_{\mathrm{NAD}}}$ is weakening, the lobe then briefly ventures over Asia and then extends down into the western Pacific, all the while preserving a positive anomaly in the central Pacific. During this time, the negative inclination anomaly centred on Hawaii persists, but is surrounded by developing regions of positivity over Australasia and the Americas. Note, however, that the magnitude of the inclination anomalies over the Americas and Asia is considerably reduced relative to earlier times. Around AD 400, the North American flux lobe re-asserts itself, there follows a trade-off of relative power in the flux lobes with extension of a third lobe down over Africa through AD 1000. Associated with this, the positive anomaly beneath Hawaii begins to weaken, ultimately to be replaced by a weaker negative anomaly around AD 1600. As this occurs, the Pacific inclination anomaly structure changes too, with the negative anomaly evolving to two foci on Hawaii and MesoAmerica (AD 700), the Hawaiian anomaly gradually dying down, becoming weakly positive around AD 1100 as a strong negative MesoAmerican–Atlantic inclination anomaly develops. Strongest positive inclination anomalies move eastward from Africa into the equatorial Indian Ocean from AD 900 to AD 1200. By AD 1300 these anomalies diminish, change sign, and, at AD 1500, there is a strong negative anomaly over Australasia, with a positive one (not as pronounced) in Africa and the Atlantic gradually moving over South America as time evolves.

Overall, we can see from figure 3 that $B_{r_{\mathrm{NAD}}}$ and inclination anomalies tend to change together at equatorial and mid-latitudes, as expected from the way in which they sample the CMB. However, inclination is much less sensitive to variations in B_r at high latitudes; thus, changes in position and relative magnitude of the flux lobes tend to be manifest as lower-latitude changes in inclination anomaly. In contrast, the largest values of declination occur at high latitudes. There is some tendency for lines of zero declination to fall close to the territory occupied by the flux lobes at high latitude. This is to be expected if the flux lobes form the major contribution to the dipole part of the geomagnetic field. It is also clear that at times when one flux lobe clearly dominates the field structure, for example between 1000 BC and 500 BC, the declination pattern is much less complex than when a pair of lobes is visible.

It is evident from figure 3 that the flux lobes are not restricted to the North American and Siberian locations that dominate the historical field models. From AD 200 to AD 300 they invade the western Pacific, and from 900 AD to 1000 AD and again from AD 1500 to AD 1700 there are large negative anomalies in $B_{r_{\mathrm{NAD}}}$ over African longitudes. However, the central Pacific seems to be exempt from such invasions, although there is substantial secular variation in the region.

4. Synthesis of results

We summarize the information contained in the 29 models of figure 3 by calculating the average properties of the field over the past 3 kyr and the variability about this mean. In figure 4 we present the average and standard deviation about the mean for each of the non-axial-dipole radial magnetic field at the CMB, the inclination anomalies, and the declinations for the 29 time samples shown in figure 3. The averages of figure $4a, c, e$ differ somewhat from those presented for ALS3K in figure 1:

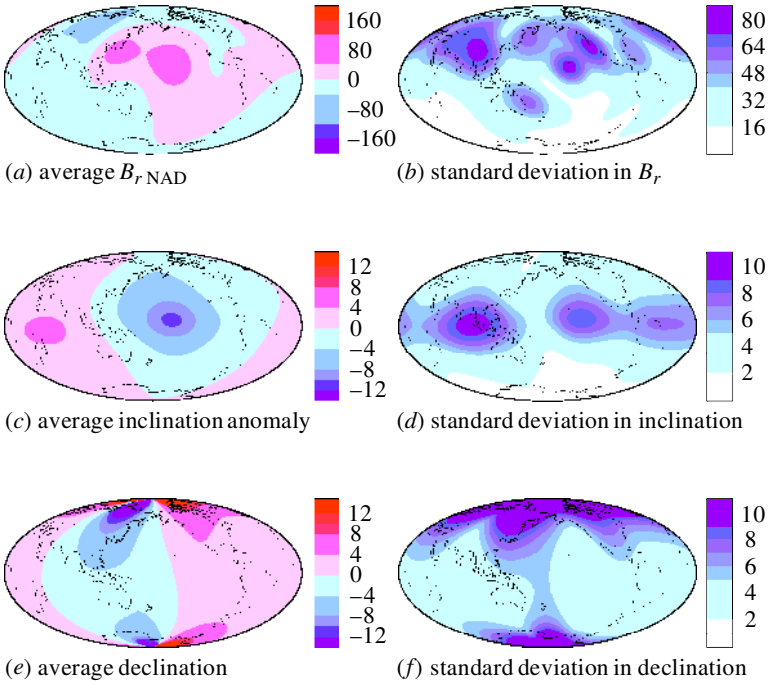

Figure 4. Average and standard deviation for $B_{r\,\mathrm{NAD}}$, (*a*), (*b*); inclination anomalies (*c*), (*d*); and declination for the models of figure 3. $B_{r\,\mathrm{NAD}}$ is in mT, inclination and declination in degrees.

this reflects the fact that ALS3K was constructed using the time-averaged data and different data uncertainties assigned earlier in our assessment of the Lund & Constable (2000) dataset, rather than averaging the predictions of the field models after their construction. Figure 2 shows that a number of sites (particularly in the Southern Hemisphere) are missing data at a significant fraction of the possible times. In the individual 100-year interval models, the absent sites will result in a stronger influence of the regularization implicit in the modelling procedure: this regularization attempts to make the model more like that for a geocentric axial dipole. The differences between figures 1*f–h* and 4*a*, *c*, *e* reflect the increasingly smooth models resulting from these data dropouts.

On average between 1000 BC and AD 1800, the Asian flux lobe dominates at northernmost latitudes; the positive anomaly in $B_{r\,\mathrm{NAD}}$ beneath Hawaii is also persistent, as is a smaller anomaly beneath Japan. At the Earth's surface, average inclination anomalies are large and negative in the central Pacific, and most positive slightly to the east of Central Africa. Inclination anomalies decrease with increasing latitude. Average declinations are smallest in equatorial regions, again with strong longitudinal variations, largest negative departures are centred over Australia and eastern Asia.

Intensity of secular variation at the Earth's surface is quantified here by standard deviation of the model inclinations and declinations about their average values, and at the CMB by standard deviation in radial magnetic field. These globally varying measures of secular variation can be compared with predictions from statistical palaeosecular variation models, like those of Constable & Johnson (1999), although we should keep in mind the temporal and spatial limitations of the data coverage.

Figure 4*b* shows the geographic variation in standard deviations in B_r at the CMB. The Southern Hemisphere is generally much less active than the Northern Hemisphere, probably a reflection of the much better northerly data coverage. Johnson & Constable (1998) show that the data used here have adequate coverage for sampling the radial magnetic field at the CMB between *ca.* 40° S and 80° N, when all sites are present. More interestingly, there are regions with good data coverage in the Northern Hemisphere, over central North America, and eastern Asia with comparatively little variation. These and other Northern Hemisphere features may well represent geographic variations in the secular variation at the CMB over the past 3 kyr. Peaks in variation in B_r occur just south of the locations of the Siberian and North American flux lobes, with a lesser maximum near the African lobe. The region beneath and slightly south of Hawaii is also a hotbed of activity. The relative importance of the Australasian region may be exaggerated by poor sampling elsewhere in the Southern Hemisphere.

Turning now to standard deviation in inclination in figure 4*d*, we see generally larger values near the Equator, as predicted by palaeosecular variation (PSV) model CJ98, with a general decrease towards the poles. Again there is less variability in the Southern Hemisphere. Significant non-zonal structure is evident in the three foci of inclination anomalies strung in a broad band around the Equator, centred in the northern Indian Ocean, southeast of Hawaii, and the central Atlantic. These anomalies are similar to the structure predicted by the non-zonal version of Constable & Johnson's (1999) statistical model for PSV (CJ98.nz). One of them even occurs in the same position, although the simple non-zonal structure assumed for CJ98.nz (based on excess variance in h_2^1 terms of the spherical harmonic expansion) is probably not an adequate representation for field variability given that the flux lobes in the 0–3 kyr interval are not confined to North America and Asia. These peaks in SV for inclination show a general correspondence with those in $B_{r_{\mathrm{NAD}}}$ in figure 4*b*, and seem to show a trilobate structure approximately coinciding with the positions occupied by flux lobes in figure 3. Declination variations (figure 4*f*) also appear trilobate, but, in contrast, are almost out of phase with B_r and inclination, reflecting the fact that the kernel for declination changes sampling B_r at the CMB is most strongly peaked at longitudes displaced 22° from the site.

5. Conclusions

The above discussion and figures 3 and 4 indicate substantive secular variation in the Pacific hemisphere over the 0–3 kyr period and suggest that the historically low secular variation in the Pacific compared with that in the Atlantic is a short-lived phenomenon. Indeed, the standard deviations in inclination anomaly, declination and $B_{r_{\mathrm{NAD}}}$ are typically larger in magnitude than the average departures from an axial-dipole field. These observations lay to rest the idea (e.g. Runcorn 1992) that an excellent conductor at or near the CMB throughout the Pacific region permanently attenuates the magnetic field changes occurring in the core field and prevents such changes from being propagated to the Earth's surface. From these models, we can conclude that the North American and Siberian flux lobes cannot be considered permanent features; however, we do see that a dominant flux lobe is almost always present somewhere in the Northern Hemisphere, and that the Asian position dominates the average for the past 3 kyr. The fact that these lobes do not occur in

the central Pacific, combined with the non-zonal structures seen in the measures of secular variation in figure 4*b*, *d*, *f*, leaves the possibility for geographic variations in heat flux at the CMB influencing the structure of the geomagnetic field wide open.

The models presented in figures 3 and 4 can be obtained by anonymous ftp from ozzy.ucsd.edu from the directory /pub/Holocene/Models.

This work was funded by NSF grants EAR 95-26890, EAR 95-26682 and EAR 93-04186.

References

Arnou, J. M., Buttles, J. L., Neumann, G. A. & Olson, P. 1996 Electromagnetic core–mantle coupling and paleomagnetic reversal paths. *Geophys. Res. Lett.* **23**, 2705–2708.

Bloxham, J. 1998 Geodynamo modelling, the paleosecular variation, and thermal core–mantle interactions. *Eos* **79**, F232.

Bloxham, J. & Jackson, A. 1992 Time-dependent mapping of the magnetic field at the core–mantle boundary. *J. Geophys. Res.* **97**, 19 537–19 563.

Bloxham, J., Gubbins, D. & Jackson, A. 1989 Geomagnetic secular variation. *Phil. Trans. R. Soc. Lond.* A **329**, 415–502.

Brito, D., Arnou, J. & Olson, P. 1999 Can heterogeneous core–mantle electromagnetic coupling control geomagnetic reversals? *Phys. Earth Planet. Interiors* **112**, 159–170.

Carlut, J. & Courtillot, V. 1998 How complex is the time-averaged geomagnetic field over the last 5 million years? *Geophys. J. Int.* **134**, 527–544.

Clark, R. M. 1975 A calibration curve for radiocarbon dates. *Antiquity* **XLIX**, 251–266.

Constable, C. G. & Johnson, C. L. 1999 Anisotropic paleosecular variation models: implications for geomagnetic field observables. *Phys. Earth Planet. Interiors* **115**, 35–51.

Constable, S. C., Parker, R. L. & Constable, C. G. 1987 Occam's inversion: a practical algorithm for generating smooth models from electromagnetic sounding data. *Geophys.* **52**, 289–300.

Daly, L. & LeGoff, M. 1996 An updated and homogeneous world secular variation database. 1. Smoothing of the archeomagnetic results. *Phys. Earth Planet. Interiors* **93**, 159–190.

Glatzmaier, G. A., Coe, R. S., Hongre, L. & Roberts, P. H. 1999 The role of the Earth's mantle in controlling the frequency of geomagnetic reversals. *Nature* **401**, 885–890.

Gubbins, D. 1998 Interpreting the plaeomagnetic field. In *The core mantle boundary region* (ed. M. Gurnis, M. E. Wysession, E. Knittle & B. Buffett), pp. 167–182. Geodynamics, vol. 28. American Geophysical Union.

Gubbins, D. & Kelly, P. 1993 Persistent patterns in the geomagnetic field over the past 2.5 Myr. *Nature* **365**, 829–832.

Holme, R. 2000 Electromagnetic core–mantle coupling. III. Laterally varying mantle conductance. *Phys. Earth Planet. Interiors* **117**, 329–344.

Hongre, L., Hulot, G. & Khokhlov, A. 1998 An analysis of the geomagnetic field over the past 2000 years. *Phys. Earth Planet. Interiors* **106**, 311–335.

Hulot, G., Khokhlov, A. & Le Mouël, J. L. 1997 Uniqueness of a mainly dipolar magnetic field recovered from directional data. *Geophys. J. Int.* **129**, 347–354.

Johnson, C. L. & Constable, C. G. 1995 The time-averaged geomagnetic field as recorded by lava flows over the past 5 Myr. *Geophys. J. Int.* **122**, 489–519.

Johnson, C. L. & Constable, C. G. 1996 Paleosecular variation recorded by lava flows over the last 5 Myr. *Phil. Trans. R. Soc. Lond.* A **354**, 89–141.

Johnson, C. L. & Constable, C. G. 1997 The time-averaged geomagnetic field: global and regional biases for 0–5 Ma. *Geophys. J. Int.* **131**, 643–666.

Johnson, C. L. & Constable, C. G. 1998 Persistently anomalous Pacific geomagnetic fields. *Geophys. Res. Lett.* **25**, 1011–1014.

Kelly, P. & Gubbins, D. 1997 The geomagnetic field over the past 5 Myr. *Geophys. J. Int.* **128**, 315–330.

Lithgow-Bertelloni, C. & Richards, M. A. 1998 The dynamics of cenozoic and mesozoic plate motions. *Rev. Geophys.* **36**, 27–78.

Lund, S. P. 1996 A comparison of holocene paleomagnetic secular variation records from North America. *J. Geophys. Res.* **101**, 8007–8024.

Lund, S. P. & Constable, C. G. 2000 Global geomagnetic secular variation for the past 3000 years. *Geophys. J. Int.* (In preparation.)

McElhinny, M. W. & McFadden, P. L. 1997 Paleosecular variation for the past 5 Myr based on a new generalized database. *Geophys. J. Int.* **131**, 240–252.

McElhinny, M. W., McFadden, P. L. & Merrill, R. T. 1996*a* The time averaged paleomagnetic field 0–5 Ma. *J. Geophys. Res.* **101**, 25 007–25 027.

McElhinny, M. W., McFadden, P. L. & Merrill, R. T. 1996*b* The myth of the Pacific dipole window. *Earth Planet. Sci. Lett.* **143**, 13–22.

Proctor, M. R. E. & Gubbins, D. 1990 Analysis of geomagnetic directional data. *Geophys. J. Int.* **100**, 69–77.

Quidelleur, X., Valet, J.-P., Courtillot, V. & Hulot, G. 1994 Long-term geometry of the geomagnetic field for the last 5 million years; an updated secular variation database from volcanic sequences. *Geophys. Res. Lett.* **21**, 1639–1642.

Richards, M. A. & Engebretson, D. C. 1992 Large scale mantle convection and the history of subduction. *Nature* **355**, 437–440.

Runcorn, S. K. 1992 Polar path in geomagnetic reversals. *Nature* **356**, 654–656.

Schneider, D. A. & Kent, D. V. 1988 Inclination anomalies from Indian Ocean sediments and the possibility of a standing non-dipole field. *J. Geophys. Res.* **93**, 11 621–11 630.

Schneider, D. A. & Kent, D. V. 1990 The time-averaged paleomagnetic field. *Rev. Geophys.* **28**, 71–96.

Walker, A. D. & Backus, G. E. 1996 On the difference between the average values of B_r^2 in the Atlantic and Pacific hemispheres. *Geophys. Res. Lett.* **23**, 1965–1968.